

Spin Accumulation in Gold Films

Mark Johnson

Bellcore, 331 Newman Springs Road, Red Bank, New Jersey 07701-7040

(Received 19 October 1992)

The spin injection technique has been used to study the transport of spin polarized conduction electrons in gold films, and has resulted in the unique observation of a large "spin bottleneck" effect. Furthermore, the measured spin diffusion length is surprisingly long.

PACS numbers: 72.15.Gd, 73.40.-c, 75.50.Rr

The transport of spin polarized conduction electrons in metals has been a continuing topic of study in condensed matter physics. The earliest technique, conduction electron spin resonance, relied on a static magnetic field and microwave excitation to create nonequilibrium populations of electron spins in bulk metal samples [1]. In a seminal experiment [2] by Tedrow and Meservey, the quasiparticle density of states of a thin Al film was Zeeman split by a static magnetic field, and tunneling conductance measurements made with a contiguous ferromagnetic film demonstrated that electrons which tunneled from the ferromagnetic film were spin polarized. This led to the discovery that the nonequilibrium spin population created by transmission electron spin resonance could be enhanced by coating the metal samples with ferromagnetic films [3]. This was followed by a demonstration of the spin injection technique [4] in which a dc current driven through a ferromagnetic film into a bulk metal sample was spin polarized; this created a population of nonequilibrium spins that diffused a distance of order 0.1 mm and was detected by another ferromagnetic film used as a spin detector. Most recently, in a related field, there have been advances in the development of a spin polarized scanning tunneling microscope [5].

This Letter presents a new development, a study of spin transport and diffusion in metal films. By adapting the spin injection methodology to a novel geometry, the study of spin dynamics is extended to a new regime, and a technique that can be applied to numerous novel systems is demonstrated. Gold films were studied because there is no prior measurement of the conduction electron spin relaxation time T_2 in gold, nor in any metal film, by electron spin resonance or other suitable technique. A spin relaxation time for electrons in polycrystalline gold films is herein deduced, but more importantly this study has discovered that the nonequilibrium spin density created in this system is much larger than has been observed in any other system, and is even larger than is predicted by theory. This unusual result will have implications for topics in such fields as magnetism, and weak localization and mesoscopic transport.

The technique is presented conceptually in Fig. 1. We consider a pedagogical model of an unconventional, three terminal device, shown in cross section in Fig. 1(a). A paramagnetic metal film P is sandwiched between two

ferromagnetic films, $F1$ and $F2$. Each ferromagnetic film is a single domain and is thin enough such that its axis of magnetization is constrained to lie in the plane of the film. A dc current is driven through $F1$ into P and returned to the current source from the bottom of P . A single voltage probe is attached to $F2$ (its ground will be discussed below), and we consider the case where the thickness d of P is less than a spin depth, $\delta_s = (2DT_2)^{1/2}$ (with D the electronic diffusion constant), the distance that spin polarized electrons can diffuse in P without losing their spin orientation. An understanding of steady state transport in this system is aided by considering the density of state diagrams of Fig. 1(b), where $F1$ and $F2$ are represented as transition metal ferromagnets in a simplified band model, P is represented as a free electron metal, and for simplicity the interfacial resistance between the films has been neglected [6].

In the absence of an imposed current, the Fermi levels E_F of all three films align at $E_{F,0}$. When a current is driven from $F1$ into P , only one spin subband in $F1$ is available to carry the current because transport involves only electrons within the energy range $k_B T$ of E_F . It fol-

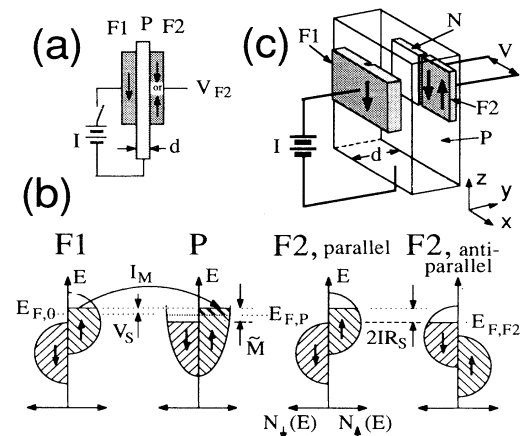


FIG. 1. (a) Pedagogical model of three terminal device. Arrows in $F1$ and $F2$ refer to magnetization orientation as determined by majority spin subband. (b) Diagrams of the densities of state, $N(E)$, of the ferromagnet-paramagnet-ferromagnet system depicted in (a). (c) The geometry used to measure V_{F2} . P is depicted transparent.

lows that a current of magnetization, $I_M = \eta_1 \beta I_e / e$ [7], is associated with the electric current I_e . Here β is the Bohr magneton (the magnetic moment carried by each electron), e is the electronic charge, and η is a phenomenological factor [4] which describes the efficiency of transport of magnetic dipoles, $\eta = (J_{\uparrow} - J_{\downarrow}) / (J_{\uparrow} + J_{\downarrow})$, where $J_{\uparrow, \downarrow}$ are current densities for each spin subband. In our pedagogical model $\eta_1 = 1$, but more generally $|\eta| \leq 1$.

In the steady state, spins enter P at a rate I_M and are lost, by random relaxation, at a rate $1/T_2$. The result is a nonequilibrium magnetization given by [4] $\tilde{M} = I_M T_2 / Ad$ where A is the area of electrode $F1$ and Ad is the volume occupied by the spins. The depiction of \tilde{M} in Fig. 1(b) conserves charge neutrality. Thus, the electric current driven through $F1$ acts as a "spin pump" which drives a nonequilibrium density of spins into P . In turn, this nonequilibrium magnetization in P has a back effect on $F1$: The chemical potential of $F1$ rises so that the chemical potential of its up-spin subband aligns with that of the up-spin subband of P . This effect has been called a spin bottleneck [8] because a thermodynamic force associated with the presence of the nonequilibrium spins [6] impedes the flow of spins into P . Because charge and spin are transported by the same carrier, it follows that the electrical impedance of the $F1$ - P interface is increased by the presence of \tilde{M} . The increase is identified in the figure (and calculated below) as $R_s = V_s / I_e$.

When the magnetization of $F2$ is parallel with that of $F1$, its chemical potential will also rise so that the chemical potential of its up-spin subband aligns with that of the up-spin subband of P . This change of chemical potential has been derived [4,9] to be $eV_s = \eta_2 \beta \tilde{M} / \chi$, where χ is the Pauli paramagnetic susceptibility of P . Some physical insight to this result can be gained by noting that \tilde{M} / χ has the units of magnetic field and can be thought of as the effective magnetic field associated with the nonequilibrium spins. Then $\beta \tilde{M} / \chi$ is the Zeeman energy of a spin polarized electron in the presence of the field associated with all of the nonequilibrium polarized spins. If the magnetization of $F2$ is antiparallel with that of $F1$, then its chemical potential lowers [$E_{F, F2}$ in Fig. 1(b)] so that the chemical potential of its down-spin subband aligns with that of the down-spin subband of P . Combining the above expressions for I_M , \tilde{M} , and V_s , and using a free electron expression for the susceptibility, $\chi = \beta^2 N(E_F) = \beta^2 3n / 2E_F$, where n is the density of conduction electrons, gives the result

$$R_s \equiv \frac{V_s}{I_e} = \frac{\eta_1 \eta_2}{e^2} \frac{T_2 E_F}{1.5nAd} = \eta_1 \eta_2 \frac{\rho \delta_s^2}{2Ad}, \quad (1)$$

where the second form results from using an Einstein relation for the electrical resistivity, $\rho = 1/e^2 DN(E_F)$.

We note that V_s is a linear function of current so that R_s has units of impedance, and that the magnitude of R_s is inversely proportional to the sample dimensions A and d . This follows from the fact that magnetization has di-

mensions of magnetic dipoles per unit volume, so that a constant number of nonequilibrium spins will result in a larger value of \tilde{M} when the volume is diminished. In addition, recall that Eq. (1) was derived for the *thin limit* case, $d < \delta_s$. The density of nonequilibrium spins decreases exponentially as a function of thickness, $\tilde{M} \propto e^{-d/\delta_s}$, so that a measurement of the diminished value of V_{F2} at thicknesses $d > \delta_s$ gives a direct measurement of δ_s .

In order to measure the floating voltage V_{F2} it is necessary to define a ground. A convenient choice is depicted in Fig. 1(c); V_{F2} is measured with respect to a normal metal counterelectrode N whose chemical potential is always aligned with the average chemical potential of P [$E_{F, P}$ in Fig. 1(b)]. To measure changes of V_{F2} associated with V_s it is necessary to manipulate the magnetizations of the ferromagnetic films. In the scheme of Fig. 1(c), $F1$ and $F2$ will have slightly different coercivities, $H_{c,1}$ and $H_{c,2}$, due to the aspect ratios associated with their different shapes [Fig. 2(a)]. Thus, the detected voltage V as a function of externally applied field H should be positive whenever the magnetizations of $F1$ and $F2$ are aligned and negative, over a field range $H_{c,2} - H_{c,1}$, when antialigned [Fig. 2(b)]. This effect was demonstrated in the original spin injection experiment [4].

The samples were fabricated on sapphire substrates. The ferromagnetic films $F1$ and $F2$ of four samples were composed of permalloy, which was deposited in a vacuum of $\sim 10^{-6}$ torr by e -beam evaporation from a single source of $\text{Ni}_{79}\text{Fe}_{21}$, and had thicknesses of 70 nm. A fifth sample used permalloy for $F1$ and Co for $F2$. The coercivities of test films of permalloy and Co were of order 10 G. The gold films were deposited by thermal evaporation from 5-9's gold after cleaning the permalloy base electrode with an Ar ion mill. The geometry was defined using photolithography and liftoff to create "windows" in insulating films of Al_2O_3 . These windows had area $A = 10^{-2} \text{ mm}^2$. The voltage measurements were made with two rf SQUID [10] amplifiers, and one of these was calibrated by measuring the resistance of a gold wire. This calibration also verified the polarity of the voltage

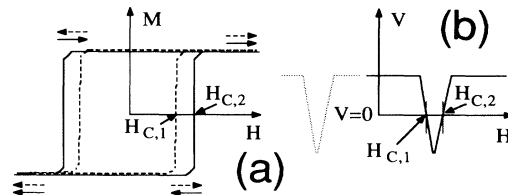


FIG. 2. (a) Hysteresis loops for $F1$ (dashed) and $F2$ (solid). Arrows represent parallel and antiparallel orientations of $F1$ and $F2$. (b) Expected shape of signal: Solid line, sweeping up in field; dotted line, sweeping down [along the top portion of the loop in (a)].

measurements.

An example of data from a film with $D=1.6 \mu\text{m}$ is shown in Fig. 3(a), with an expanded view presented in Fig. 3(b). The signals were linear with current over the experimental range, typically 0.1 to 10 mA, and voltages of order 10^{-8} V were recorded. The dynamic range of the SQUID voltmeters is 10^{-7} V and this was the only limit to the voltage magnitudes observed. The shape, width, and sign of the data of Fig. 3 conform to the expectations of a spin injection signal [Fig. 2(b)]. Similar signals were recorded for sweeps of magnetic field along \hat{x} and \hat{z} . The nonzero median value is consistent with a slight asymmetry in the placement of the windows $F2$ and N [refer to Fig. 1(c)]. All samples showed nonzero offsets that ranged from several $\mu\Omega$ to several $\text{m}\Omega$, but typically were a few tens of $\mu\Omega$. For one sample this offset was less than R_s , so that the observed signal was bipolar. Another confirmation of the spin injection model was achieved in the following way. A constant field of about 30 G was applied in the \hat{x} direction, and a sweep was performed along \hat{z} . Under this condition the magnetizations of $F1$ and $F2$ reorient from $-\hat{z}$ to $+\hat{z}$ by rotating towards \hat{x} , and the magnetizations are never antiparallel. As expected, the narrow dips at $\pm H_c$ disappeared.

Because the coercivities of $F1$ and $F2$ are so close in value the spin-coupled signal is observed only over a small range $H_{c,2} - H_{c,1} \approx 4$ G. The observed signals must represent a lower limit of the actual value of R_s because it is not possible to know whether the films are completely antiparallel. Despite this possible source of error, the signals were quite reproducible (typically $\pm 25\%$) and consistent from sample to sample. Another source of error results from the existence of magnetic anisotropies (easy or hard axes of magnetization) in the films. For example, the small "hump" at $H=18$ G suggests that anisotropies

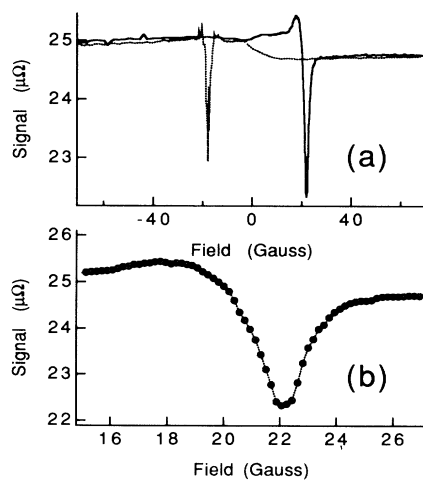


FIG. 3. (a) An example of data: Solid line, sweeping up in field; dotted line, sweeping down. (b) Expanded view: $d=1.6 \mu\text{m}$; $I=4.0$ mA.

exist which prevent the films from aligning completely when $H = \pm 70$ G. When H approaches H_c the magnetizations briefly come closer to alignment before one film flips its magnetization to antiparallel alignment. Magnetization measurements of a test film confirmed the existence of in-plane anisotropies of order 10 G, and an anisotropy in the \hat{y} direction was observed in the Co film. Finally, two samples show broad undulations over a field range of 40–50 G (i.e., about $2H_c$), centered at $H=0$. These broad features are believed to be associated with the "spin bottleneck" and magnetization states of $F1$ that vary locally in the vicinity of $F2$ and N , and are not believed to affect the magnitude of the narrow dips at $\pm H_c$.

From Eq. (1) we see that the magnitude of R_s is proportional to the parameters η and T_2 . While η should be temperature independent, the simplest picture of spin scattering in metals suggests that any scattering event has a small, constant probability a_s of flipping a spin, and therefore $T_2^{-1} \propto \tau^{-1} = a_s \tau^{-1}$ where τ is a scattering time derived from Matthiessen's rule. For bulk Al, for example, a_s has the value [4] $a_{s,\text{Al}} \approx 1 \times 10^{-3}$. It follows that $R_s \propto \tau$, and in this approximation $R_s(T)$ should have the same temperature dependence as the electrical conductivity σ of the gold, which also is linearly proportional to τ . Figure 4(a) demonstrates the comparable temperature dependence of $R_s(T)$ and $\sigma(T)$ over the experimental range $4 \text{ K} < T < 65 \text{ K}$, and furthermore suggests that the signals should not be greatly diminished at room temperature.

The expression in Eq. (1) predicts that the product $R_s A d$ should be constant as a function of d , for thicknesses $d < \delta_s$. This scaling is demonstrated in Fig. 4(b), where the open symbols refer to comparable sam-

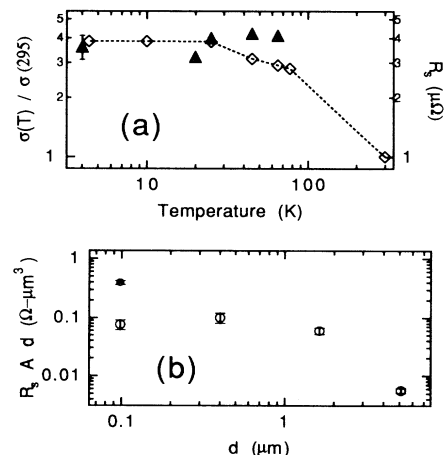


FIG. 4. (a) Comparison of $\sigma(T)$ (left axis; open diamonds) with $R_s(T)$ (right axis; closed triangles). (b) $R_s A d$ as a function of d . R_s is referred to the current through a single "window." Open symbols, $F1$ and $F2$ are permalloy; closed symbol, $F2$ is Co.

ples ($F1$ and $F2$ are both permalloy). The analyses of Figs. 4(a) and 4(b) further confirm the spin injection model. It is interesting to note, in Fig. 4(b), that the resistance across the thickness of the $1.6 \mu\text{m}$ thick film is about $1.3 \mu\Omega$, somewhat smaller than the $3 \mu\Omega$ spin-coupled impedance (refer to Fig. 3), but of the same order of magnitude. However, the resistance across the gold film decreases linearly with decreasing thickness d whereas R_s increases in proportion to $1/d$. Thus, at a thickness of about 100 nm the spin-coupled voltage is 3 to 4 orders of magnitude larger than the resistive voltage drop.

The spin depth may be determined by fitting the data of Fig. 4(b) by Eq. (1) in the thin limit, $d < 1 \mu\text{m}$, and by the thick limit form [11], $R_s = (\eta_1 \eta_2 \rho \delta_s / 2A) e^{-d/\delta_s}$, for $d > 1 \mu\text{m}$. The best fit gives the result $\delta_s = 1.5 \pm 0.4 \mu\text{m}$. The spin relaxation time can be calculated from the expression $\delta_s = (2DT_2)^{1/2} \approx [2(v_F^2 \tau / 3) T_2]^{1/2}$, where v_F is the Fermi velocity. Using a Drude time for τ one finds, for the temperature range $4 \text{ K} < T < 65 \text{ K}$, $T_2 = (1.7 \pm 0.9) \times 10^{-11} \text{ sec}$, and $a_{s,\text{Au}} \approx 6 \times 10^{-3}$. It is noteworthy that the ratio τ/T_2 is comparable with that of bulk metal.

A comparison can now be made between the observed magnitude of the effect and that predicted by Eq. (1). Using the above value for T_2 , the largest magnitude predicted, for the optimum value $|\eta| = 1$ [12], is $R_s A d \approx 9 \times 10^{-3} \Omega \mu\text{m}^3$. However, the signals in permalloy-Au-permalloy samples are about 9 times larger, and in the permalloy-Au-Co sample it is about 40 times larger, than predicted by theory. I note that the theory has used a simplified expression for χ , and has neglected many-body effects. Furthermore, electric current in the volume Ad that has already undergone spin relaxation may experience spin flip interactions at the F - P interface (interactions which repolarize the spins) as it diffuses out of the sample region. This "reentrant" effect may be a source of signal enhancement in the thin limit.

The theory of spin relaxation in metals suggests that the spin orbit interaction in gold should be the dominant spin scattering effect and predicts a high scattering probability [13] $a_{s,\text{Au}} = 5 \times 10^{-2}$. The observed probability $a_{s,\text{Au}} = 6 \times 10^{-3}$ is significantly smaller than expected, but is in good agreement with weak localization studies [14] of gold films which have measured a ratio $\tau/\tau_{\text{so}} = 8 \times 10^{-3}$, where τ_{so} is the spin orbit scattering time. I note that τ_{so} is not identically the same as T_2 , though T_2 should approach τ_{so} in the limit of strong spin orbit interactions, and that τ_{so} was measured in films with extreme disorder, a somewhat different regime from that of

the experiments described herein. The surprisingly long value measured for T_2 remains one of the intriguing results of this study.

In summary, I have adapted the spin injection technique to a novel geometry to study the transport of spin polarized conduction electrons in gold films. This study demonstrated the utility of the spin injection technique, and suggests the possibility of studying spin excitations and spin transport in novel systems such as superconductors (metals and cuprates), semiconductors, spin glasses, and two-dimensional electron gases.

The author is grateful to G. Prinz for a critical reading of the manuscript.

-
- [1] Freeman Dyson, Phys. Rev. **98**, 349 (1955); Richard B. Lewis and Thomas R. Carver, Phys. Rev. **155**, 309 (1967).
 - [2] P. M. Tedrow and R. Meservey, Phys. Rev. Lett. **26**, 192 (1971); Phys. Rev. B **7**, (1973); R. Meservey *et al.*, Phys. Rev. Lett. **37**, 858 (1976).
 - [3] R. H. Silsbee, A. Janossy, and P. Monod, Phys. Rev. B **19**, 4382 (1979).
 - [4] Mark Johnson and R. H. Silsbee, Phys. Rev. Lett. **55**, 1790 (1985); Phys. Rev. B **37**, 5312 (1988); **37**, 5326 (1988).
 - [5] Mark Johnson and John Clarke, J. Appl. Phys. **67**, 6141 (1990); R. Weisendanger *et al.*, Phys. Rev. Lett. **65**, 247 (1990).
 - [6] Mark Johnson and R. H. Silsbee, Phys. Rev. B **35**, 4959 (1987); see the appendix for the fully generalized solution.
 - [7] A. G. Aronov, Pis'ma Zh. Eksp. Teor. Fiz. **24**, 37 (1976) [Sov. Phys. JETP Lett. **24**, 32 (1976)].
 - [8] Mark Johnson, Phys. Rev. Lett. **67**, 3594 (1991).
 - [9] R. H. Silsbee, Bull. Magn. Res. **2**, 284 (1980); see also Ref. [4].
 - [10] Commercial SQUID from B.T.I.
 - [11] Mark Johnson and R. H. Silsbee, Phys. Rev. Lett. **58**, 2806 (1987).
 - [12] Values of η for comparable permalloy films were 0.45 in Ref. [2] and 0.05 in Ref. [4].
 - [13] Y. Yafet, in *Solid State Physics*, edited by F. Seitz and D. Turnbull (Academic, New York, 1963), Vol. 14, p. 1. Use a form similar to Eq. (20.3), note that the g shift δg is first order in the spin orbit splitting Δ_{nl} , and use values of Δ_{nl} and ΔE from Table II to compute T_2/τ for Au relative to that for Na (which is calculated explicitly in Sec. 21).
 - [14] G. Bergmann, Z. Phys. B **48**, 5 (1982); Phys. Rep. **107**, 2 (1984).